Computer Science Journal of Moldova, vol.**20**, no.2(59), 2012

# Medical Image Registration by means of a Bio-Inspired Optimization Strategy

Hariton Costin, Silviu Bejinariu

**Abstract**

Medical imaging mainly treats and processes missing, ambiguous, complementary, redundant and distorted data. Biomedical image registration is the process of geometric overlaying or alignment of two or more 2D/3D images of the same scene, taken at different time slots, from different angles, and/or by different acquisition systems. In medical practice, it is becoming increasingly important in diagnosis, treatment planning, functional studies, computer-guided therapies, and in biomedical research. Technically, image registration implies a complex optimization of different parameters, performed at local or/and global levels. Local optimization methods frequently fail because functions of the involved metrics with respect to transformation parameters are generally nonconvex and irregular. Therefore, global methods are often required, at least at the beginning of the procedure. In this paper, a new evolutionary and bio-inspired approach – bacterial foraging optimization – is adapted for single-slice to 3-D PET and CT multimodal image registration. Preliminary results of optimizing the normalized mutual information similarity metric validated the efficacy of the proposed method by using a freely available medical image database.

**Keywords:** medical imaging, image registration, soft computing, evolutionary strategies, bacterial foraging algorithm, global optimization.

## 1 Introduction

Image registration (IR) is a fundamental task in computer vision used to find either a spatial *transformation* (e.g., rotation, translation, etc.)

or a correspondence (matching of similar image entities) among two (or more) images taken under different conditions (at different times, using different sensors, from different viewpoints, or a combination of them), with the aim of overlaying such images into a common one [Gon02], [Pra01], [Ran05]. Over the years, IR has been applied to a broad range of situations from remote sensing to medical images or artificial vision and CAD systems, and different techniques have been independently studied resulting in a large body of research.

IR methods can be classified in two groups according to the nature of images [Cor06]: *voxel*-based IR methods (also called *intensity*-based), where the whole image is considered for the registration process; and, on the other side, *feature*-based methods, which consider prominent information extracted from the images, being a reduced subset of them. The latter methods take advantage of the lesser amount of information managed in order to overcome the problems found in the former when the images present some inconsistences to deal with, for example, regardless of changes in the geometry of the images, radiometric conditions, and appearance of noise and occlusion. These features correspond to *geometric primitives* (points, lines, surfaces, etc.) which are invariant to the transformation to be considered between the input images. Moreover, the latter methods perform faster than the former ones due to the reduced amount of data they take into account, at the expense of achieving *coarse* results.

Likewise, IR is the process of finding the optimal spatial transformation (e.g., rigid, similarity, affine, etc.) achieving the best overlaying between two (or more) different images named *scene and model* images (Figure 1). They both are related with the specific transformation, measured by a *similarity metric* function. Such transformation estimation is interpreted into an iterative optimization procedure in order to properly explore the search space. Two search approaches have been considered in the IR literature: *matching-based*, where the optimization problem is intended to look for a set of correspondences of pairs of those more similar image entities in both the scene and the model images, from which the registration transformation is derived; and the *transformation parameter-based*, where the strategy is to directly explore

inside each range of the transformation parameters. Both strategies can be used with either a voxel-based or a feature-based approach.

Specific aspects such as the presence of noise, image discretization, different amplitudes in the scale of the IR transformation parameters, the magnitude of the transformation to be estimated cause difficulties for traditional local optimizers (gradient- and nongradient-based) and they become prone to be trapped in local minima. As a consequence, global methods are preferred, at least at the beginning of the IR process.

***Medical imaging modalities***

Within the current clinical setting, medical imaging is a vital component of a large number of applications occurring throughout the clinical track of events, e.g. in clinical diagnostic, planning, consummation, and evaluation of surgical and radiotherapeutical procedures.

The imaging modalities can be divided into two global categories, i.e. *anatomical* and *functional*. Anatomical modalities include X-ray, CT (computed tomography), MRI (magnetic resonance imaging), US (ultrasound), and (video) sequences obtained by various catheter "scopes".

Functional modalities depict primarily information on the metabolism of the specific anatomy. They include scintigraphy, SPECT (single photon emission computed tomography), PET (positron emission tomography), which all are *nuclear medicine* imaging modalities, then fMRI (functional MRI), pMRI (perfusion MRI), fCT (functional CT), EIT (electrical impedance tomography), and MRE (magnetic resonance elastography).

Since information gained from two images acquired in the clinical practice is usually of a complementary nature, proper *integration* of useful data obtained from the separate image modalities is often desired. A first step in this integration process is to bring the modalities involved into spatial alignment, a procedure referred to as *registration*. After registration, a *fusion* step may be required for the integrated display of the data involved.

## 2 The image registration problem

During the last decades, hundreds of papers were dedicated to image registration (IR) problem and different taxonomies have been established to classify the IR methods presented so far, considering different criteria: the image acquisition procedure, the search strategy, the type of transformation relating the images, and so forth [Mai98], [Zit03], [Zol03]. There is not a universal design for an IR method that could be applicable to all registration tasks, since various considerations on the particular application must be taken into account.

Yet, IR methods usually require the four following components (Figure 1): two input *Images*, named as Scene $Is = \{p_1, p_2, ..., p_n\}$ and Model $Im = \{p_1, p_2, ..., p_m\}$, with $p_i$ and $p_j$ being image points; a *registration transformation* $f$ being a parametric function relating the two images; a *similarity metric function* $F$ in order to measure a qualitative value of closeness or degree of fitting between the transformed scene image, denoted by $f'(Is)$, and the model image; and an *optimizer* which looks for the optimal transformation $f$ inside the defined solution search space. Hence, the key idea of the IR process is focused on determining the unknown parametric *transformation* that relates both images, by placing them in a common coordinate system bringing the points as close as possible. Of course, the global optimum is obtained at the best registration transformation. Because of the uncertainty underlying such transformation, the IR task arises as a *nonlinear problem* that cannot be solved by a direct method (e.g., resolution of a simple system of linear equations). It should be solved by means of an iterative procedure searching for the *optimal estimation* of $f$, following a specific search space optimization scheme aiming at minimizing the error of a given *similarity metric* of resemblance. Classical local optimizers can be used for this task although their main drawback is that they usually get trapped in a local minima solution. The main reasons for such behavior are related to both the nature of the problem to be tackled and the greedy/local search features of these methods. So, the interest on the application of soft-computing and Artificial Intelligence in general to the IR optimization process has increased in the last decade due to

their global optimization nature.

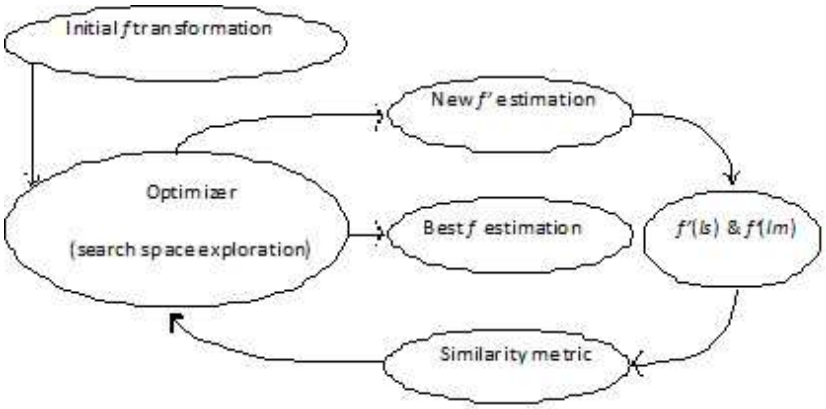


Figure 1. Image registration as an optimization process

According to the nature of images, IR methods can be classified as *voxel*-based (or *intensity*-based) and *feature*-based. The former directly operate with the whole raw images. The latter approach introduces a step before the application of the registration process: a reduced subset of the most relevant features is extracted from the images. One important drawback of voxel-based methods is that they can not reliably approach the variable contrast obtained during the acquisition of different images. In that case, the similarity metric offers unreliable measurements and often induces the optimization process to be trapped in local minima. The feature-based methods of IR are based on the extraction of salient *features* (e.g. geometric primitives) from the images. The feature detector has to accurately extract invariant features, i.e. regardless of changes in the geometry and contrast of the images and appearance of noise.

## 2.1 Transformations

The IR methods can be classified according to the registration transformation used to relate both the scene and the model images. The

first category of transformation models includes *linear transformations*, which preserves the operations of vector addition and scalar multiplication, being a combination of translation, rotation, global scaling, and shear components. The most common linear transformations are rigid, similarity, affine, projective, and curved. Linear transformations are global in nature, thus not being able to model local deformations. The second category of transformation models includes *"elastic"* or *"non-rigid"* transformations, which allow local warping of image features, thus providing support for local deformations.

## 2.2 Similarity metric

The similarity metric is a function $F$ that measures the goodness of a given registration solution, that is, of a registration transformation $f$. The final performance of any IR method strongly depends on its accurate estimation. Each solution is evaluated by $F$ applying such transformation $f$ on one of the two images, usually to the scene image ($f(I_s)$). Next, the degree of closeness or fitting between the transformed scene and the model images, $\Psi(\cdot)$ must be determined,

$$F(I_s, I_m, f) = \Psi(f(I_s), I_m). \tag{1}$$

The main approaches trying to estimate the function $\Psi(\cdot)$ depend on the dimensionality (2D or 3D) and the nature of the considered images. There are: (a) voxel-based approach: sum of squared differences, normalized cross-correlation (i.e., correlation coefficient or phase correlation), and mutual information; (b) feature-based approach: feature values-based metrics (i.e., registration based on the curvature) and distance between corresponding geometric primitives.

Unfortunately, the $F$ function is affected by both the discretization of images and the presence of noise, yielding worse estimations and favoring the IR to get trapped in local minima.

### 2.3 Search space strategies

The IR process performs an iterative exploration to obtain that optimal transformation $f$ (introduced in Figure 1). So, the closer $f$ to the unknown global optimum, the better the fitting (measured by the similarity metric $F$) between scene and model. The optimization process considered to obtain those solutions can be deterministic or stochastic (either a global or a local one).

Although the final registration problem solution consists of the right values for the parameters which determine $f$, we can distinguish two different strategies to solve the problem, each of them working in a different solution space:

(i) the first searches in the *matching space* to obtain a set of correspondences of pairs of the most similar image entities in both the scene and the model images, from which the registration transformation is derived;

(ii) the second directly makes a search in the space of the $f$ parameters guided by the $F$ function, called *transformation parameters* space.

The matching-based search space exploration usually consists of the two following stages: first, a set of correspondences with those more similar regions of pixels (voxel-based) or geometric primitives (feature-based) in both the scene and the model images must be computed; second, the transformation $f$ is assessed by numerical methods considering the previous matching.

On the contrary, transformation parameters-based search space involves directly searching for the solution in the space of parameters of the transformation $f$. In this respect, each solution to the IR problem is encoded as a vector composed of the values for the parameters of $f$, and the IR method generates possible vectors of parameter values, that is, possible registration transformations. As a consequence, the search space exploration is guided by the similarity metric $F$. In this way, each solution vector is evaluated by the chosen metric, and the

IR problem becomes a parameter optimization procedure of finding the best values of $f$ that maximize the similarity metric $F$.

Other classification divides search strategies in *local* and *global* ones. Local optimization techniques frequently fail because functions of these metrics with respect to transformation parameters are generally non-convex and irregular and, therefore, global methods – such as those based on evolutionary algorithms – are often required.

In recent years a lot of studies and papers were dedicated to medical IR [Alt06], [Coo03], [He02], [Hil94], [Lav04], [Lev08], [Mai96, 98], [Plu03], [Qin93], [Zib01], [Xua06]. Concerning the CT—PET images registration topic, some valuable attempts were made in the past. Thus, rigid 3D transformations were performed, e.g., by Alpert [Alp90] using the images principal axes and center of gravity, and by Pietrzyk [Pie94], who used a fully interactive method. Affine registration was obtained by Wahl [Wah93], employing user identified anatomical landmarks and external markers, and Maguire [Mag91], who optimized cross-correlation around such user identified anatomical landmarks and external markers. In [Lee06] a robust surface registration using a Gaussian-weighted distance map (GWDM) for PET-CT brain fusion was proposed. A similarity measure was evaluated repeatedly by weighted cross-correlation (WCC).

In recent years, the application of several well-known *evolutionary algorithms* (*EAs*) to the IR optimization process has introduced an outstanding interest in order to solve those problems due to their global optimization techniques nature. The first attempts to solve IR using evolutionary computation [Bac97] can be found in the early eighties, when Fitzpatrick et al. [Fit84] proposed such approach based on a genetic algorithm for the 2D case and applied it to angiographic images. Since then, several evolutionary approaches have been proposed to solve the IR problem, mainly in connection with the transformation parameters-based search space, as it is shown e.g. in [Cho04], [Cor06], [Cor07], [Eti00], [Rey06], [Rou00], [Wac04]. The main reason of using global optimization techniques, such as EAs-based algorithms for IR, is that they do not require an optimum solution to achieve high accuracy of registration.

## 3 Bacterial foraging algorithm

Introduced by Passino [Pas02], [Liu02], bacterial foraging paradigm is a bio-inspired optimization method based on the foraging model. This paradigm belongs to the broader class of distributed nongradient global optimization. A foraging animal takes actions to maximize the energy obtained per unit time spent for foraging, $E/T$, in the face of constraints presented by its own physiology (e.g., sensing and cognitive capabilities) and environment (e.g., density of prey, risks from predators, physical characteristics of the search area). In other words, these social animals, like E. coli – a bacterium, try to maximize their long-term average rate of energy intake.

Let us suppose that $\theta$ is the position of a bacterium and $J(\theta)$ represents the combined effects of attractants and repellants from the environment, with, for example, $J(\theta) < 0$, $J(\theta) = 0$, and $J(\theta) > 0$ representing that the bacterium at location $\theta$ is in nutrient-rich, neutral, and noxious environments, respectively. We want to find the minimum of $J(\theta)$, $\theta \in \Re^p$ , where we do not have measurements or an analytical description of the gradient $\nabla J(\theta)$. So, ideas from bacterial foraging are used to solve this nongradient optimization problem. Basically, *chemotaxis* is a foraging behavior that implements a type of optimization where bacteria try to climb up the nutrient concentration (find lower and lower values of $J(\theta)$), avoid noxious substances, and search for ways out of neutral media (avoid being at position $\theta$ where $J(\theta) \geq 0$). In this way, they implement a type of biased random walk.

The chemotactic actions of E. coli may be resumed as follows:

(i) if in neutral medium, alternate tumbles and runs $\Rightarrow$ search;

(ii) if swimming up a nutrient gradient (or out of noxious substances), swim longer (climb up nutrient gradient or down noxious gradient) $\Rightarrow$ seek increasingly favorable environments;

(iii) if swimming down a nutrient gradient (or up noxious substance gradient), then search $\Rightarrow$ avoid unfavorable environments.

### 3.1 Chemotaxis, swarming, reproduction, elimination, and dispersal

In [Pas02], [Pas05] a chemotactic step was defined to be a tumble followed by a tumble or a tumble followed by a run. Let $j$ be the index for the chemotactic step. Let $k$ be the index for the reproduction step. Let $l$ be the index of the elimination-dispersal event. Let

$$P(j,k,l) = \{\theta^i(j,k,l) \quad | \quad i = 1,2,\ldots,S\} \tag{2}$$

represent the position of each member in the population of the $S$ bacteria at the $j$th chemotactic step, $k$th reproduction step, and $l$th elimination-dispersal event. Here, let $J(i,j,k,l)$ denote the cost at the location of the $i$th bacterium $\theta^i(j,k,l) \in \Re^p$ (sometimes we may refer to the $i$th bacterium position as $\theta^i$). Note: we will interchangeably refer to $J$ as being a "cost" (using terminology from optimization theory) and as being a nutrient surface (in reference to the biological connections). For actual bacterial populations, $S$ can be very large (e.g., $S = 10^9$), but $p = 3$. In computer simulations, we may use much smaller population sizes and keep the population size fixed. Let $N_c$ be the length of the lifetime of the bacteria as measured by the number of chemotactic steps they take during their life. Let $C(i) > 0$, $i = 1,2,\ldots,S$, denote a basic chemotactic step size that we will use to define the lengths of steps during runs.

To represent a tumble, a unit length random direction, say $\phi(j)$, is generated; this will be used to define the direction of movement after a tumble. In particular, we let

$$\theta^i(j+1,k,l) = \theta^i(j,k,l) + C(i)\phi(j) \tag{3}$$

so that $C(i)$ is the size of the step taken in the random direction specified by the tumble. If at $\theta^i(j+1,k,l)$ the cost $J(i,j+1,k,l)$ is better (lower) than at $\theta^i(j,k,l)$, then another step of size $C(i)$ in this same direction will be taken. This swim is continued as long as it continues to reduce the cost, but only up to a maximum number of steps, $N_s$ . This represents that the cell will tend to keep moving if it is headed in

the direction of increasingly favorable environments. The above discussion is for the case where no cell-released attractants are used to signal other cells that they should swarm together. The cell-to-cell signaling via an attractant is represented with $J_{cc}^{i}(\theta,\, \theta^{i}(j,k,l))$, $i = 1, 2, \ldots, S$, for the $i$th bacterium.

Let $d_{attract}$ be the depth of the attractant released by the cell and $w_{attract}$ be a measure of the width of the attractant signal (a quantification of the diffusion rate of the chemical). The cell also repels a nearby cell in the sense that it consumes nearby nutrients and it is not physically possible to have two cells at the same location. To model this, we let

$$h_{repellant} = d_{attract}$$

be the height of the repellant effect and $w_{repellant}$ be a measure of the width of the repellant.

Let

$$J_{cc}(\theta, P(j,k,l)) = \sum_{i=1}^{S} J_{cc}^{i}(\theta, \theta^{i}(j,k,l)) = \tag{4}$$

$$= \sum_{i=1}^{S} \left[ -d_{attract} \exp\left( -w_{attract} \sum_{m=1}^{p} (\theta_m - \theta_m^i)^2 \right) \right]$$

$$+ \sum_{i=1}^{S} \left[ h_{repellant} \exp\left( -w_{repellant} \sum_{m=1}^{p} (\theta_m - \theta_m^i)^2 \right) \right]$$

denote the combined cell-to-cell attraction and repelling effects, where $\theta = [\theta_1, \ldots, \theta_p]^T$ is a point on the optimization domain and $\theta_m^i$ is the $m$th component of the $i$th bacterium position $\theta^i$. Note that as each cell moves, so does its $J_{cc}^{i}(\theta, \theta^{i}(j,k,l))$ function, and this represents that it will release chemicals as it moves. Due to the movements of all the cells, the $J_{cc}(\theta, P(j,k,l))$ function is time varying in that if many cells come close together there will be a high amount of attractant and hence an increasing likelihood that other cells will move toward the group. This produces the swarming effect, where the $i$th bacterium, $I = 1, 2, \ldots, S$,

will hill-climb on $J(i,j,k,l) + J_{cc}(\theta, P)$ (rather than the $J(I,j,k,l)$ defined above) so that the cells will try to find nutrients, avoid noxious substances, and at the same time try to move toward other cells, but not too close to them. The $J_{cc}(\theta, P)$ function dynamically deforms the search landscape as the cells move to represent the desire to swarm, i.e., swarming is viewed as a minimization process.

After $N_c$ chemotactic steps, a reproduction step is taken. Let $N_{re}$ be the number of reproduction steps to be taken. For convenience, we assume that $S$ is a positive even integer.

Let

$$S_r = S/2 \tag{5}$$

be the number of population members who have had sufficient nutrients so that they will reproduce (split in two) with no mutations. For reproduction, the population is sorted in order of ascending accumulated cost (higher accumulated cost represents that a bacterium did not get as many nutrients during its lifetime of foraging and hence is not as "healthy" and thus unlikely to reproduce); then the $S_r$ least healthy bacteria die and the other $S_r$ healthiest bacteria each split into two bacteria, which are placed at the same location. Other fractions or approaches could be used in place of (5); this method rewards bacteria that have encountered a lot of nutrients and allows us to keep a constant population size, which is convenient in coding the algorithm.

Let $N_{ed}$ be the number of elimination-dispersal events, and for each elimination-dispersal event each bacterium in the population is subjected to elimination-dispersal with probability $p_{ed}$. We assume that the frequency of chemotactic steps is greater than the frequency of reproduction steps, which is in turn greater in frequency than elimination-dispersal events (e.g., a bacterium will take many chemotactic steps before reproduction, and several generations may take place before an elimination-dispersal event).

The Bacterial Foraging Optimization Algorithm (BFOA) is fully described in pseudo-code in paper [Pas02] and was used as it is during our experiments.

# 4 Mutual information based multimodal image registration

Multimodal images acquired at different time moments have variations due to the acquisition system, position of the subject, and different geometric deformations. To optimally register and then fuse multimodal images, we have to minimize the linear and non-linear differences between the two images. In our paper we propose the use of *normalized mutual information* as a similarity metric for registering PET and CT images. Mutual information, which measures statistical dependence between two images viewed as random variables, has been proved to be robust for multimodal registration, with respect to dynamic range and intensity resolution of the images. Mutual information represents a measure of the relative independence of two images, in the sense that high values indicate high dependence.

Registration of multimodal medical images may be described as follows. For instance, let $P$ and $C$ be the PET and CT images for registration, respectively. *Mutual information* between the two images can be represented as

$$M(P,C) = H(P) + H(C) - H(P,C). \tag{6}$$

$H(\cdot)$ is the entropy of the image and $H(P,C)$ is the joint entropy. Registering $P$ with respect to $C$ (in this manner, as CT image has much more geometric information) requires maximization of mutual information between P and C, thus maximizing the entropy $H(P)$ and $H(C)$, and minimizing the joint entropy $H(P,C)$. Because mutual information based registration methods are sensitive to changes that occur in the distributions as a result of difference in overlapping regions, *normalized mutual information* can be used:

$$NM(P,C) = \frac{H(P) + H(C)}{H(P,C)}. \tag{7}$$

Our study approaches the *rigid body image registration*, which initially determines global alignment, followed by local elastic registration. Let $T$ denote the spatial transformation that maps features or

coordinates (spatial locations) from one image or coordinate space to another image or coordinate space. Let $p_A$ and $p_B$ denote coordinate points (pixel locations) in images $A$ and $B$, respectively. The image registration problem is to determine $T$ so that the mapping $T : p_A \rightarrow p_B \Leftrightarrow T(p_A) = p_B$ results in the "best" alignment of $A$ and $B$. For 3-D rigid body registration, the mapping of coordinates $p = [x, y, z]^T$ into $p' = [x', y', z']^T$ can be formulated as a matrix multiplication in homogeneous coordinates, as shown in (8) in an explicit manner. That is, the goal of the optimization is to determine the parameters $t_x$, $t_y$, $t_z$, $\alpha$, $\beta$, and $\gamma$ in (8).

Usually, optimization in image registration means to maximize similarity. Similarity metric values, as functions of transformation parameters, refer to *the objective function*, denoted as $f(x)$. Alternatively, one may formulate the image registration as a minimization problem and, thus, the goal is to minimize $-f(x)$. Although there is yet no proof for its optimality, because of its robustness (usually it attains its maximum at correct alignment) and good results in previous works, normalized mutual information was selected as the similarity measure in our study. Moreover, it is still generally non-smooth and prone to local optima. For this reason, global optimization approaches are preferred.

$$\begin{bmatrix} p' \\ 1 \end{bmatrix} = \mathbf{T} \begin{bmatrix} p \\ 1 \end{bmatrix} \Leftrightarrow$$
$$\begin{bmatrix} x' \\ y' \\ z' \\ 1 \end{bmatrix} = \begin{bmatrix} \cos\beta\cos\gamma & \cos\alpha\sin\gamma + \sin\alpha\sin\beta\cos\gamma & \sin\alpha\sin\gamma - \cos\alpha\sin\beta\cos\gamma & t_x \\ -\cos\beta\sin\gamma & \cos\alpha\cos\gamma - \sin\alpha\sin\beta\sin\gamma & \sin\alpha\cos\gamma - \cos\alpha\sin\beta\sin\gamma & t_y \\ \sin\beta & -\sin\alpha\cos\beta & \cos\alpha\cos\beta & t_z \\ 0 & 0 & 0 & 1 \end{bmatrix} \begin{bmatrix} x \\ y \\ z \\ 1 \end{bmatrix} \quad (8)$$

## 5 Biomedical image registration using bacterial foraging algorithm

In contrast to genetic algorithms and evolutionary strategies, which exploit the competitive characteristics of biological evolution (e.g., sur-

vival of the fittest), bacterial foraging (BF) exploits cooperative and social aspects of animal colonies (like E. coli bacterium) in their attempts to obtain nutrients that maximize energy intake per unit time spent for foraging.

As it is shown before, the registration of an image with another is seen as the minimization of the objective function of normalized mutual information (7). For a rigid body registration this means to find the transformation $\mathbf{T}$ (that is, parameters $t_x$, $t_y$, $t_z$, $\alpha$, $\beta$, and $\gamma$ in (8)) that maps the pixel $p$ into pixel $p'$.

We have chosen to register 2-D PET images into 3-D CT images, taken from www.medcyclopaedia.com, as depicted in Figure 6 and Figure 7 below. Normalized mutual information was computed using 60 histogram bins, which generally produces a smooth density approximation while retaining intensity features [Mae97]. Each 2-D image was oriented at $d_0 = 10, 15, 20, 25$, and 30 voxels from ground truth translation (relative small distances), as expert knowledge of the correct orientation can greatly help the search process. For each distance, ten orientations were applied, ranging from $5^\circ$ to $45^\circ$. For each 2-D image, distance, and orientation, eight trials were performed. After some trials, the population size was chosen to be $S = 150$.

Transform $T$ that maps the pixel $p$ in pixel $p'$ is defined by 6 parameters: $t_x$, $t_y$, $t_z$, $\alpha$, $\beta$, $\gamma$. To find the optimal transform in terms of normalized mutual information, the bacterial foraging algorithm was used for optimization in space $\Re^6$. To have a uniform treatment of the parameters, the search space was scaled in interval [0, 100] for all six parameters.

Within the bacterial foraging paradigm, the following chemotactic actions are defined:

(i) search in a neutral medium;

(ii) seek increasingly favorable environments;

(iii) avoiding unfavorable environments.

Considering that a priori information about the transform parameters is unknown, only the search case can be used. Cells-released attractants

are used to signal other cells the favorable movement directions.

In the example above, we reduced the search space to $\Re^2$ and the following parameters were used: number of bacteria in the population $S = 150$, number of chemotactic steps before reproduction – 100, magnitude of secretion of attractant $d_{attract} = 0.1$ and chemical cohesion signal $w_{attract} = 0.2$.

In Figure 2, the bacteria trajectories for the first 4 generations are presented. After 4 generations an elimination / dispersal was applied and the trajectories for the next 4 generations are shown in Figure 3.

Next, the following parameters were varied: magnitude of secretion of attractant, $d_{attract} = 0.25$ and chemical cohesion signal, $w_{attract} = 0.1$ (Figures 4 and 5). The more the chemical cohesion signal value is smaller, so the attractant is more diffused.

The validity of the proposed method was checked by means of the following metrics [Wac04]:

1) *accuracy*, as measured by the ratio of correct registrations to all registrations. A registration is considered to be correct if the Euclidean distance from the ground truth translation ($[t_{x0}, t_{y0}, t_{z0}]$) and final translation ($[t'_{x0}, t'_{y0}, t'_{z0}]$) is less than 2 voxels, and if the maximum absolute value of the three rotation errors is less than 2. These values have been found to be good indicators of registration quality; we obtained accuracies between 0.6 and 0.8 for different images; as anticipated, the best accuracies were obtained for $d_0 = 10$ voxels from ground truth translation;

2) *efficiency*, as measured by the mean number of function evaluations for correct registrations for each 2-D image registered to a 3-D volume.

The mean run time varied among different trials, between tens of seconds and 130 sec.

Moreover, registered PET-CT images are less sensitive to *contrast changes* compared to the CT images alone. As anticipated, the registered images also provide more distinguishing information compared to the PET and CT images. These properties of the proposed method

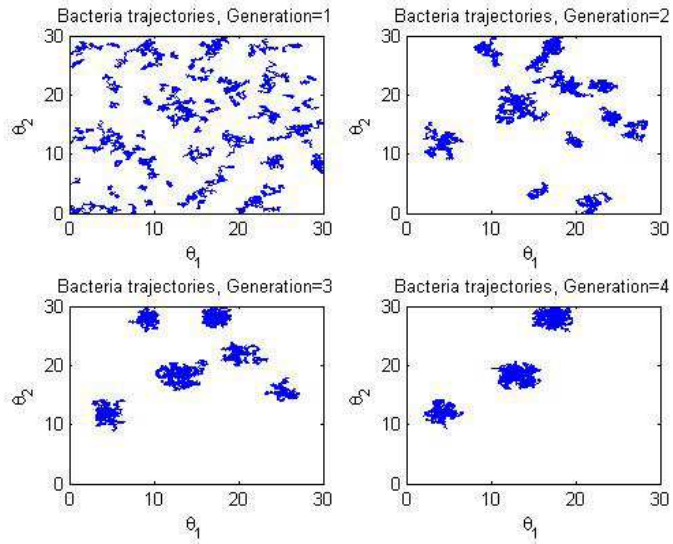


Figure 2. Bacteria trajectories for the first 4 generations $d_{attract} = 0.1$, $w_{attract} = 0.2$

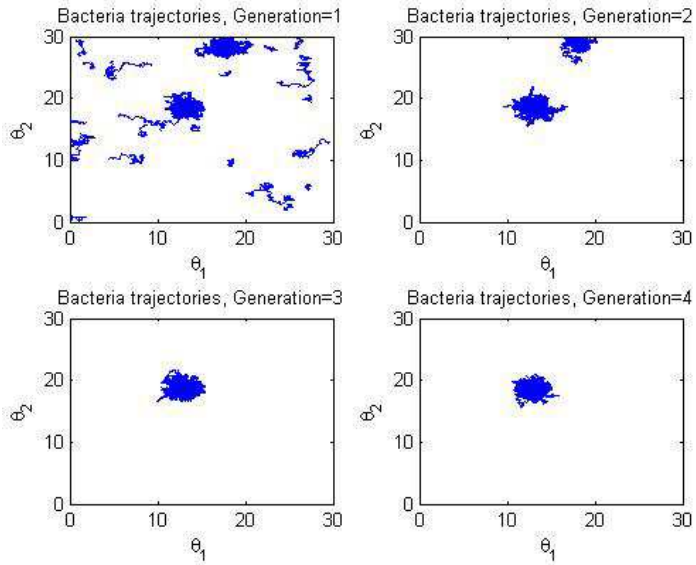


Figure 3. Bacteria trajectories for 4 generations after elimination dispersal, $d_{attract} = 0.1$, $w_{attract} = 0.2$

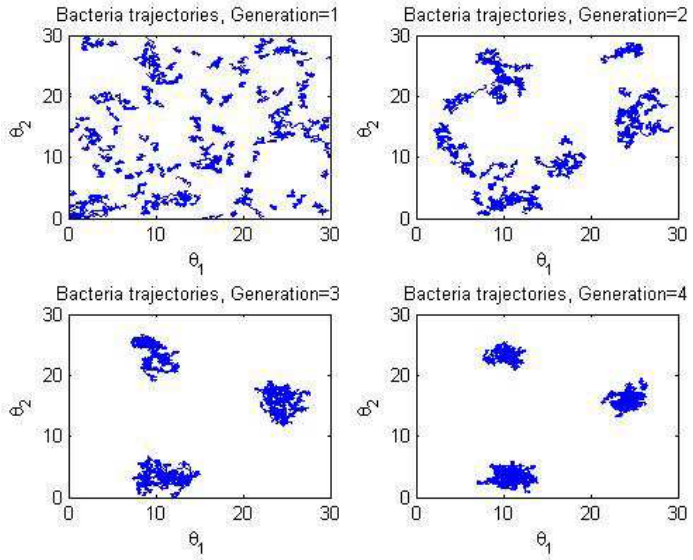


Figure 4. Bacteria trajectories for the first 4 generations $d_{attract} = 0.25$, $w_{attract} = 0.1$

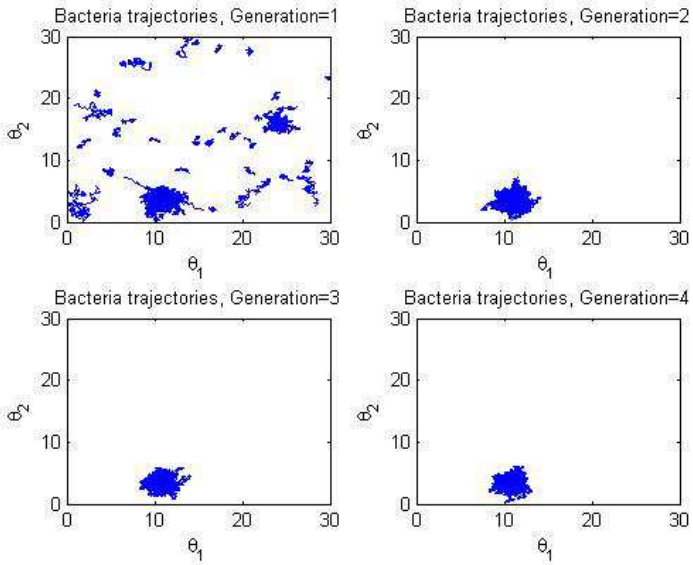


Figure 5. Bacteria trajectories for 4 generations after elimination dispersal, $d_{attract} = 0.25$, $w_{attract} = 0.1$

lead us to further continuing our study to improve the registration performance.

Figure 6 is an example of PET-CT image registration, with images taken from the portal www.medcyclopaedia.com. From medical point of view, it demonstrates the physiologic accumulation of fludeoxyglucose (FDG), a radiopharmaceutical, in the whiter regions of the body image.

In Figure 7, a coronal PET scan (b) presents an intense hypermetabolic activity shown by an arrow. This image may represent a tumor in the bowel or a mesenteric lymph node. This dilemma was later solved at biopsy, and a primary carcinoid tumor was found.

## 6 Conclusions

A new application of bacterial foraging optimization algorithm (BFOA), specifically used for biomedical image registration, was proposed in this paper. The preliminary results demonstrate the efficacy of using BF and stochastic global optimization for biomedical image registration. Moreover, like many evolutionary techniques, BFOA is intrinsically parallel, and execution times can be significantly improved by using distributed- or shared-memory computer architectures.

Concerning the actual application in medical imaging, it is already known that the primary advantage of PET-CT fusion technology is the ability to correlate findings from two complementary imaging modalities in a comprehensive way that synergetically combines anatomic information with functional and metabolic data. CT provides very fine anatomic details but does not yield functional information, whereas FDG PET lacks anatomic information but reveals aspects of different tumors and allows metabolic measurements. Yet, physiologic FDG uptake in non-malignant conditions limits the specificity of PET, particularly in the post-therapy setting. Hybrid PET-CT scanners allow PET and CT image fusion for differentiation of physiologic variants from juxtaposed or mimetic neoplastic lesions and more accurate tumor localization. However, software-based fusion of separately acquired PET and CT scans is more likely to lead to misregistration due to inde-

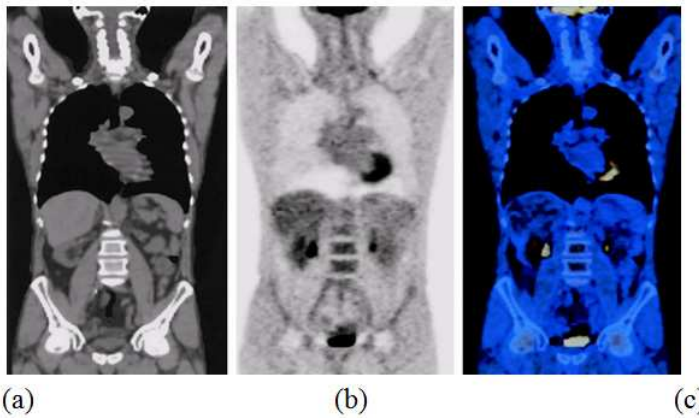


Figure 6. Coronal CT (a), PET (b), and PET-CT registered (c) images

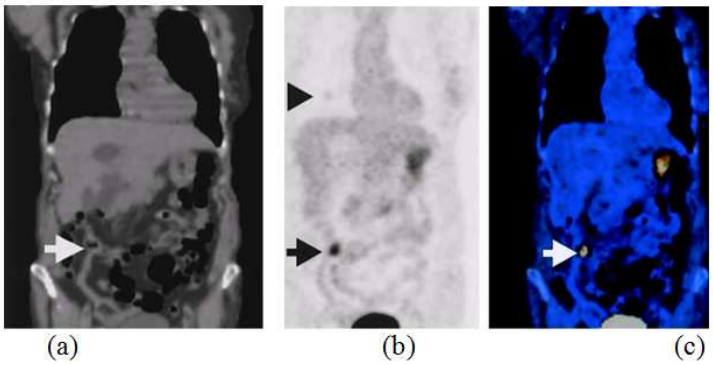


Figure 7. Primary carcinoid tumor of the bowel. CT image (a), PET image (b), and PET-CT image (c)

pendent parameters and differences in patient positioning. In addition, CT allows rapid acquisition of attenuation correction data for the PET scan.

This study shows that the accuracy obtained by image registration with BFOA is well suited for image-guided radiotherapy. Of course, we have to extend our work to annotated databases, both for PET-CT images, and for separately acquired PET and CT images.

Future work will be dedicated to combine bacterial foraging approach with other evolutionary techniques and local methods for image registration, as the need for hybrid approaches for difficult registration problems claims.

*Acknowledgment*

The authors would like to thank Prof. Ion Poiată, MD, PhD, both for the help in manually segmentation and registration of the used images, and for results evaluation during our experiments.

## References

[1] [Alp90] N.M. Alpert, J.F. Bradshaw, D. Kennedy, and J.A. Correia. *The principal axis transformation – a method for image registration*, Journal of nuclear medicine, **31**, 1717–1722, 1990.

[2] [Alt06] R. Alterovitz, *et al. Registration of MR prostate images with biomechanical modeling and nonlinear parameter estimation*, Medical Physics, vol. 33, no. 2, pp. 446–454, Feb. 2006.

[3] [Bac97] T. Back, D. B. Fogel, and Z. Michalewicz, Eds. *Handbook of Evolutionary Computation*, IOP, Bristol, UK; Oxford University Press, Oxford, UK, 1997.

[4] [Cho04] C. K. Chow, H. T. Tsui, and T. Lee. *Surface registration using a dynamic genetic algorithm*, Pattern Recognition, vol. 37, no. 1, pp. 105–117, 2004.

[5] [Coo03] J. Cooper. *Optical flow for validating medical image registration*, Proc. of the 9th IASTED Int. Conference on Signal and Image Processing, IASTED/ACTA Press, pp. 502–506, 2003.

[6] [Cor06] O. Cordon, S. Damas, and J. Santamara. *Feature-based image registration by means of the CHC evolutionary algorithm*, Image and Vision Computing, vol. 24, no. 5, pp. 525–533, 2006.

[7] [Eti00] E.K. Etienne and M. Nachtegael, (eds.). *Fuzzy Techniques in Image Processing*, Physica-Verlag, N.Y., 2000.

[8] [Gon02] R.C. Gonzales and R.E. Woods. *Digital Image Processing* ($2^{nd}$ Ed.), Prentice Hall, New Jersey, 2002.

[9] [He02] R. He and P. A. Narayana. *Global optimization of mutual information: application to three dimensional retrospective registration of magnetic resonance images*, Computerized Medical Imaging and Graphics, vol. 26, no. 4, pp. 277–292, 2002.

[10] [Hil94] D. Hill, C. Studholme, and D. Hawkes. *Voxel similarity measures for automated image registration*, Proceedings of the Third SPIE Conference on Visualization in Biomedical Computing, 1994, pp. 205–216.

[11] [Lav04] W.C. Lavavely, C. Scarfone, et al. *Phantom validation of co-registration of PET and CT for image-guided radiotherapy*, Medical Physics, 31(5), pp. 1083–92, 2004.

[12] [Lee06] Ho Lee and Helen Hong. *Robust surface registration for brain PET-CT fusion*, in Medical Imaging 2006: Visualization, Image-Guided Procedures, and Display, Ed. by Cleary, Kevin R.; Galloway, Robert L., Jr., Proceedings of the SPIE, Vol. 6141, pp. 684–693, 2006.

[13] [Lev88] D.N. Levin, C.A. Pelizzari, *et al. Retrospective geometric correlation of MR, CT, and PET images*, Radiology, 169(3), pp. 817–823, 1988.

[14] [Liu02] Y. Liu and K.M. Passino. *Biomimicry of social foraging bacteria for distributed optimization: models, principles, and emergent behaviors*, Journal of Optimization Theory and Applications, Vol. 115, No. 3, pp. 603–628, December 2002.

[15] [Mae97] F. Maes, A. Collignon, et al., *Multimodality image registration by maximization of mutual information*. IEEE Trans. Med. Imaging, 16(2), pp. 187–198, 1997.

[16] [Mag91] G.Q. Maguire, M. Noz, *et al. Graphics applied to medical image registration*. IEEE Computer graphics and applications, 11(2), pp. 20–28, 1991.

[17] [Mai96] B.A. Maintz, P.A. van den Elsen, and M.A. Viergever. *Registration of SPECT and MR brain images using a fuzzy surface*, in Loew, M. H. and Hanson, K. M. (eds), *Medical Imaging: Image processing*, Vol. 2710, pp. 821–829, Bellingham, WA. SPIE, 1996.

[18] [Mai98] B.A. Maintz, M.A. Viergever. *A survey of medical image registration*, Medical Image Analysis, volume 2, number 1, pp 1–37, Oxford University Press, 1998.

[19] [Med] www.medcyclopaedia.com

[20] [Pas02] K.M. Passino. *Biomimicry of Bacterial Foraging for Distributed Optimization and Control*, IEEE Control Systems Magazine, pp. 52–67, June 2002.

[21] [Pas05] K.M. Passino. *Biomimicry for Optimization, Control, and Automation*, Chapter 18. Cooperative Foraging and Search, Springer Verlag, 2005.

[22] [Pie96] U. Pietrzyk, K. Herholz, et al. *Clinical applications of registration and fusion of multimodality brain images from PET*, SPECT, CT, and MRI. European Journal of Radiology, 21, pp. 174–182, 1996.

[23] [Plu03] J.P. Pluim, J.B.A. Maintz, and M.A. Viergever. *Mutual information-based registration of medical images: a survey*, IEEE Transactions on Medical Imaging, 22(8), pp. 986–1004, 2003.

[24] [Pra01] W.K. Pratt. *Digital Image Processing*, John Wiley & Sons, New York, 2001.

[25] [Pub] http://pubimage.hcuge.ch:8080/

[26] [Qin93] Qin-Sheng Chen. *Image Registration and its Applications in Medical Imaging*, PhD thesis, Vrije Universiteit Brussel, 1993.

[27] [Ran05] R.M. Rangayyan. *Biomedical Image Analysis*, CRC Press, Boca Raton, 2005.

[28] [Rey06] M. Reyes-Sierra and C. A. Coello Coello. *Multi-objective particle swarm optimizers: a survey of the state-of-the-art*, International Journal of Computational Intelligence Research, Vol. 2, No. 3, pp. 287–308, 2006.

[29] [Rou00] J.-M. Rouet, J.-J. Jacq, and C. Roux. *Genetic algorithms for a robust 3-D MR-CT registration*, IEEE Trans. on Information Technology in Biomedicine, **4**, no. 2, pp. 126–136, 2000.

[30] [Zit03] Barbara Zitova and J. Flusser. *Image registration methods: a survey*. Image and Vision Computing, Elsevier, 21, pp. 977–1000, 2003.

[31] [Zol03] L. Zöllei, J. Fisher, and W.M. Wells. *A unified statistical and information theoretic framework for multi-modal image registration*, Information Processing in Medical Imaging (IPMI), LNCS 2732, pp. 366–377, 2003.

[32] [Zib01] M. Zibaeifard and M. Rahmati. *An improved multi-stage method for medical image registration based on mutual information*, Proceedings of the Eighth International Conference on Computer Vision, pp. 718–725, 2001.

[33] [Xua06] J. Xuan, Y. Wang, et al. *Nonrigid medical image registration by finite-element deformable sheet-curve models*, Int. Journal of Biomedical Imaging, Volume 2006, Article ID 73430, pp. 1–9, Hindawi Publishing Corporation.

[34] [Wac04] M. P. Wachowiak, Renata Smolíková, et al. *An approach to multimodal biomedical image registration utilizing particle swarm optimization*, IEEE Transactions on Evolutionary Computation, Vol. 8, No. 3, pp. 289–301, June 2004.

[35] [Wah93] R.L. Wahl, L.E. Quint, et al. *"Anametabolic" tumor imaging: fusion of FDG PET with CT or MRI to localize foci of increased activity.* Journal of nuclear medicine, 34, pp. 1190–1197, 1993.

Hariton COSTIN[1,2], Silviu BEJINARIU[2],

Received June 20, 2012

[1]Faculty of Medical Bioengineering,
"Grigore T. Popa" Univ. of Medicine and Pharmacy,
Iaşi, Romania;
Str. M. Kogalniceanu No. 9-13, 700454,
Iaşi, Romania

[2] Institute of Computer Science of Romanian Academy,
Iaşi Branch, B-dul Carol I No. 11, 700506,
Iaşi, Romania,
E–mail: *hcostin@gmail.com*